Caucasian Journal of Science
ISSN: 2148-6840
https://doi.org/ 10.48138/cjo.1404252
Year: 2023
Volume: 10 Issue: 2

**To Cite:** Turhan, Z. Ş., Öztürk, E. & Karakoyun, N. (2023). Quantum Chemical Studies of Sensitizers Designed for Dye-Sensitive Solar Cells. Caucasian Journal of Science, 10(2), 162-182.

# Quantum Chemical Studies of Sensitizers Designed for Dye-Sensitive Solar Cells

Zeynep Şilan TURHAN[1], Erhan ÖZTÜRK[2], Necdet KARAKOYUN[3]

**Kimya / Chemistry** **Araştırma Makalesi / Research Article**

## Makale Bilgileri

**Geliş Tarihi**
13.12.2023
**Kabul Tarihi**
29.12.2023

**Anahtar Kelimeler**
DFT,
Boyaya duyarlı güneş pilleri,
Optoelektronik,
Fotovoltaik özellikler,
TD-DFT

## Öz

Bu çalışmada, D-π1-π2-A yapısına (E3-E4) sahip E0 referans boyasından D-π1-R-π2-A yapısına sahip iki farklı organik boya tasarlandı. Referans boya E0 üzerindeki π köprüleri arasına 2,3-disyanopirirazinofenantren eklenerek ve π köprüsü değiştirilerek, boyaya duyarlı güneş pili (DSSC) cihazlarında kullanılmak üzere fotovoltaik özellikleri incelemek üzere tasarlanan boyalar elde edildi. Tasarlanan boyaların geometrik yapıları, absorpsiyon spektrumları, Doğrusal Olmayan Optik özellikleri (NLO'lar), enerji seviyeleri, sınır moleküler yörüngeleri ve bazı fotovoltaik ve kimyasal reaktivite parametreleri gibi çeşitli özellikleri, Boyaya Duyarlı Güneş Pillerinin (DSSC'ler) performansını artırmak için Yoğunluk Fonksiyonel Teorisi (DFT) ve zaman bağımlı DFT (TD-DFT) yöntemleri kullanılarak araştırıldı. Hesaplanan teorik sonuçlar, tasarlanan boyalardan E4'ün, E0'a kıyasla yüksek kısa devre akımına ve daha iyi güç dönüşüm enerjisine (PCE) sahip olabileceği sonucuna varıldı. Bu sonuçlar, farklı yardımcı ligandların eklenmesinin ve π-köprülerinin değiştirilmesinin sistemin fotovoltaik performansını etkili bir şekilde artırabileceğini göstermektedir.

## Article Info

**Received**
13.12.2023
**Accepted**
29.12.2023

**Keywords**
DFT,
Dye-sensitized solar cells,
Optoelectronics,
Photovoltaic properties,
TD-DFT

## Abstract

In this study, two different organic dyes with a D-π1-R-π2-A structure were designed from the reference dye E0 with a D-π1-π2-A structure (E3-E4). By adding 2,3-dicyanopyrirazinophenanthrene between the π-bridges on the reference dye E0 and changing the π-bridge, dyes designed to examine the photovoltaic features for use in dye-sensitized solar cell (DSSC) devices were obtained. Various properties of the designed dyes, such as their geometrical structures, absorption spectra, Nonlinear Optical properties (NLOs), energy levels, boundary molecular orbitals, and some photovoltaic and chemical reactivity parameters, were investigated using Density Functional Theory (DFT) and time-dependent DFT (TD-DFT) methods to improve the performance of Dye-Sensitized Solar Cells (DSSCs). The calculated theoretical results concluded that E4 of the designed dyes can have a high short-circuit current and better power conversion energy (PCE) compared with E0. These results indicate that adding different auxiliary ligands and modifying the π-bridges can effectively improve the photovoltaic performance of the system.

---

[1] Igdır University, Faculty of Science and Literature, Department of Biochemistry, Igdır/ Turkey; e-mail: zeynepsilanturhan@hotmail.com; ORCID: 0000-0002-3587-2576

[2] Igdır University, Research Laboratory Practice and Research Center (ALUM), Igdır/Turkey; e-mail: kimyagerhan@hotmail.com; 0000-0003-4006-2428 (Corresponding author)

[3] Van Yuzuncu Yil University, Muradiye Vocational High School, Department of Chemistry and Chemical Management Technologies, Van/Turkey; e-mail: necdetkarakoyun@yyu.edu.tr; 0000-0002-6083-6921

## INTRODUCTION

The sun is a vital source of renewable energy, providing life-sustaining opportunities for all living beings on our planet. The most important advantage of the energy obtained from the sun is that it is sustainable and environmentally friendly. The energy obtained from the sun can be converted into electricity. Electrical energy is the most easily obtainable and usable form of energy. For this reason, studies are being carried out today to generate electricity economically from solar energy (Kumar et al., 2015).

Solar cells are analyzed into three different groups according to their structure and construction. First-generation solar cells are single and multilayer crystalline silicon solar cells. The second generation is produced from thin film. The third generation is dye-sensitized organic solar cells. Dye-sensitized organic solar cells have drawn significant attention in scientific research due to their many advantages, including streamlined manufacturing, cost-effectiveness and exceptional cell efficiency, since they were originally published by Grätzel and O'Regan in 1991 (Grätzel, 2001; Hamann et al., 2008; O'regan & Grätzel, 1991). A typical DSSC device is composed of four important components: a semiconductor anode (typically made of $TiO_2$), a sensitizer, counter electrodes, and potential redox electrolytes. Figure 1 provides a visual representation of these components (Higashino & Imahori, 2015; Liang & Chen, 2013).

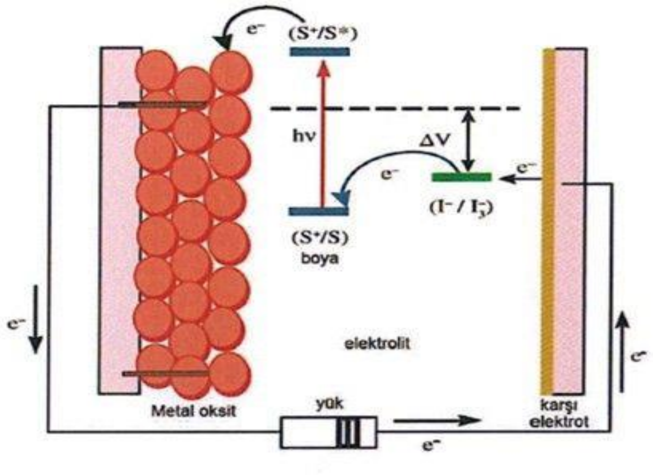

**Figure 1.** Schematic of the DSSC

Although there have been significant developments in solar cell technology recently, studies should be carried out on the high cost of solar cell production, and the cost should be reduced. DSSCs are being intensively investigated as a renewable energy source due to their low cost and efficiency at large wavelengths of light (Higashino & Imahori, 2015; Tan et al., 2014).

The sensitizer in DSSC devices is one of the most significant chemicals, and its value lies in the absorption and conversion of sunlight into electricity (Li et al., 2019). Sensitizers can be classified into two main categories: those are metallic and non-metallic organic sensitizers. Among sensitizers, metallic compounds show the highest conversion energy efficiencies, achieving up to 11% for Ru complexes and 13% for Zn porphyrins (Figure 2) (Bomben et al., 2012; Mathew et al., 2014).

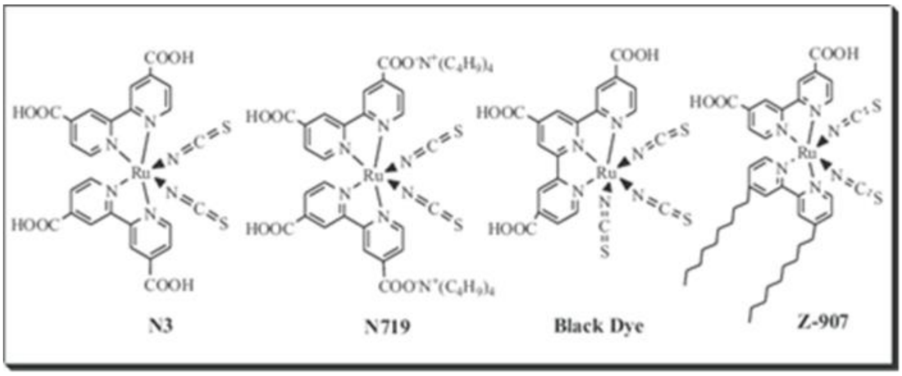

**Figure 2.** Structure of N3, N719, black dye, and Z-907 sensitizer

In order to enhancing the Optimising the sensitizer's performance is essential to raising the power conversion efficiency (PCE) of DSSC devices (Slimi et al., 2020) and (Higashino & Imahori, 2015; Tan et al., 2014). Metal-free organic sensitizers are becoming popular due to their advantages, such as easy synthesis and purification, higher extinction coefficients, eco-friendliness, programmable energy levels, and optical characteristics (Huang et al., 2020; Yang et al., 2018). Generally, D-π-A structures with the donor (D) and acceptor (A) connected by the π-bridge are the best non-metallic organic sensitizers for DSSC applications (Dutta et al., 2020). The optoelectronic performance of organic dye sensitizers with D-π-A configurations is enhanced due to their enhanced charge separation and increased intramolecular charge transfer (ICT) mechanism between donors (D) and acceptors (A) via the π-bridge (Li et al., 2020b; Mandal et al., 2020).

The optoelectronic properties of organic dyes can be efficiently customized through structural modifications to electron-rich donors and electron-deficient acceptors, which is made possible by the extension of the π-bridge (Singh & Kanaparthi, 2022). Researchers expanded the π-conjugated bridge with thiophene to create non-metallic organic dyes to enhance the the photovoltaic performance of DSSCs Zang et al. (Zhang et al., 2017). The

HOMO-LUMO energy gap is significantly reduced and strong planarity is produced when the length of the π-bridge is increased, as demonstrated by theoretical simulations employing DFT and TD-DFT in comparison to the reference dye BZTP-1. According to the computed findings, all of the developed dyes have excellent electron injection and dye regeneration characteristics, which can increase the photovoltaic characteristics and energy conversion efficiency of the sensitizers.

Noh et al. (2021) To attain excellent photovoltaic efficiency for application in dye solar cells, we theoretically studied novel dyes and synthesized them utilizing auxiliary π-extended acceptor units. The findings of this study demonstrate that the DSSC-based engineered dye SGT-60 possesses a higher PCE of 10.28% as compared to the reference dye SGT-130 with a PCE of 10.06%. This indicates that extending π-conjugation is advantageous in enhancing the photovoltaic performance of sensitizers.

Ho et al. (Ho et al., 2021) synthesized a range of organic dyes (5a, 5b, 5c, 8a, 8b, and 8c), with dye 8a having the highest PCE of 5.25%. (Figure 3).

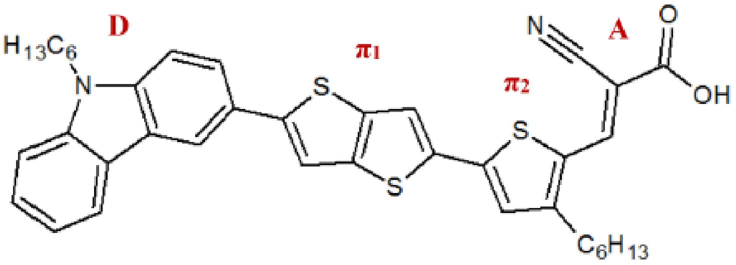

**Figure 3.** Reference dye molecular structure (Ho et al., 2021)

Britel et al. (Britel et al., 2023b) created new dyes in order to identify acceptable dyes with enhanced PCE for usage as sensitizers in DSSCs with improved photovoltaic efficiency (M1-M7); 8a is designated as M1. They used density function theory (DFT) and time-dependent DFT (TD-DFT) methodologies to theoretically study how to increase the performance of the DSSC. Because of their extremely tiny energy gaps, broad absorption spectra, good NLO characteristics, and low reorganization energies ($\lambda_{tot}$), the proposed dyes can be employed as possible sensitizers in DSSCs, according to the theoretical results. In comparison to the reference dye, M1 had a lower regeneration driving force ($\Delta G_{reg}$), a longer stimulated duration (τ), a greater vertical dipole moment (μnormal), a reasonable electron injection driving force ($\Delta G_{inj}$), and an equally reasonable light harvesting efficiency (LHE). It was also discovered that the reference dye M1 has a lower power conversion energy (PCE) and a lower short-circuit current than the developed dyes (M2-M8) due to their superior charge transferability, greatest stabilisation energy, and maximum electron-donating and electron-accepting abilities. These findings demonstrated that the installation of various auxiliary receivers Ai may most effectively increase the system's photovoltaic performance.

In this study, 8a from Ho et al. (Ho et al., 2021) was taken as a reference and named **E0**. From the reference dye **E0** with a D-π1-π2-A structure, two different organic dyes with a D-π1-R-π2-A structure were designed (**E3–E4**) (Figure 4). Dyes designed for dye-sensitized solar cells (DSSC) devices were obtained by adding 2,3-dicyanopyrirazinophenanthrene between the π-bridges on the reference dye **E0** and changing the π-bridge to study the photovoltaic properties. Density function theory (DFT) and time-dependent DFT (TD-DFT) were used to theoretically investigate the geometrical structures, absorption spectra properties, nonlinear optical properties (NLOs), energy levels, boundary molecular orbitals, and some photovoltaic parameters of the designed dyes in order to improve the DSSC performance.

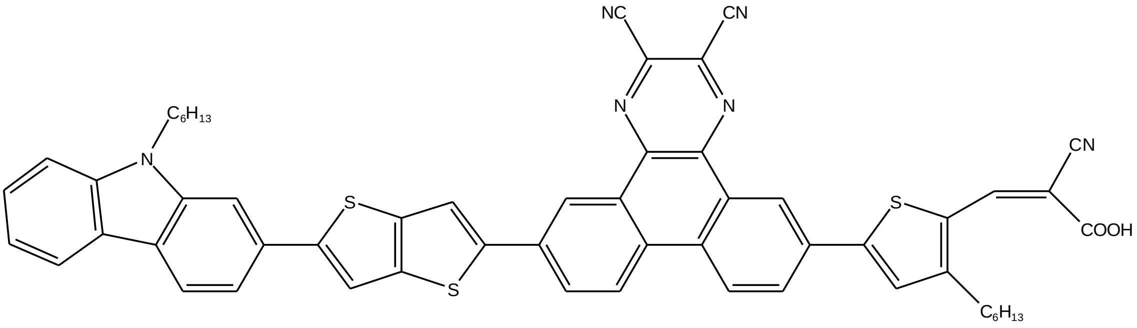

E3

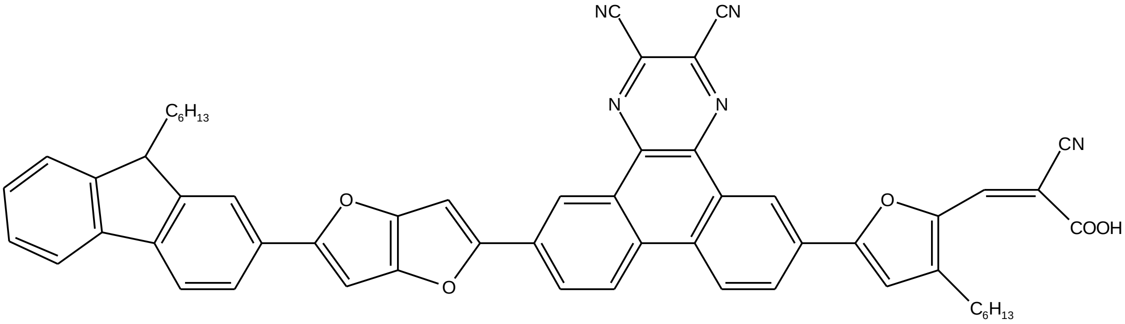

E4

**Figure 4.** 2D structures of the designed dyes

## Calculation Methods

### Theoretical Background

Power conversion efficiency (PCE) is an important statistic for assessing a molecule's performance in a DSSC device. Equation 1 may be used to calculate PCE (Ibrahim et al., 2021):

$$PCE = \frac{J_{sc}V_{oc}}{P_{inc}}FF \tag{1}$$

where $J_{sc}$, $V_{oc}$, FF, and $P_{inc}$ denote short circuit current density, open circuit voltage, filling factor, and incident solar energy.

The following is the $J_{sc}$ expression for DSSC (Mersal et al., 2021):

$$J_{sc} = \int LHE\ (\lambda)\phi_{inj}\ \eta_{coll}\, d\lambda \tag{2}$$

In Equation 2, LHE is the light collection efficiency, $\phi_{inj}$ is the electron injection efficiency, and $\eta_{coll}$ is the charge collection efficiency. It can be assumed that $\eta_{coll}$ is constant for the same DSSCs with different dyes. To improve $J_{sc}$, the dye should have high LHE, $\phi_{inj}$, and small reorganization energy.

Equation 3 is used to compute the LHE of the dyes under consideration (Marlina et al., 2022):

$$LHE = 1 - 10^{-f} \tag{3}$$

where ƒ is the oscillator power at a dye's maximal wavelength.

$\phi_{inj}$ is determined by the electron injection driving force ($\Delta G_{inj}$), which can be calculated as follows (Tripathi et al., 2022):

$$\Delta\, G_{inj} = E_{dye*} - E_{CB} = \left( E_{dye} - E_{ex} \right) - E_{CB} \tag{4}$$

$E_{dye*}$ is the excited dye's oxidation potential energy, and $E_{dye*}$ is the dye's ground state oxidation potential energy, which may be calculated as the negative of the energy of the highest occupied molecular orbital ($E_{HOMO}$) (Roohi & Mohtamadifar, 2022). $E_{CB}$ is the reduction potential of the conduction band (CB) of the semiconductor $TiO_2$ ($E_{CB}$ = -4.0 eV) and $E_{ex}$ is the vertical transition energy associated with $\lambda_{max}$ (Fitri et al., 2014b).

The reorganization energy of the vacancy ($\lambda_h$), electron ($\lambda_e$), and total ($\lambda_{tot}$) is calculated by the following relations (Fitri et al., 2014a):

$$\lambda_e = ( E_0^- - E_-^- ) + ( E_-^0 - E_0^0 ) \tag{5}$$

$$\lambda_h = ( E_0^+ - E_+^+ ) + ( E_+^0 - E_0^0 ) \tag{6}$$

$$\lambda_{tot} = \lambda_h + \lambda_e \tag{7}$$

In Equations 5 and 6, $E_0^-$ ($E_0^+$) is the anion (cation) energy computed using the optimised neutral molecule; $E_-^-$ ($E_+^+$), is the an anion (cation) energy computed with the optimized neutral molecule; $E_-^0$ ($E_+^0$), is the computed energy of the neutral molecule in the anion (cation) state; and $E_0^0$ is the neutral molecule's ground-state energy.

Moreover, the ability of the oxidized dye to retrieve an electron from the electrolyte after light stimulation is known as dye regeneration ($\Delta G_{reg}$). $\Delta G_{reg}$ should be smaller for a faster electron transfer process, as suggested by the driving force of dye regeneration. This can be computed as follows (Saad Ebied et al., 2022):

$$\Delta G_{reg} = E_{I^- / I_3^-} - E_{dye} \tag{8}$$

Here $E_{I^- / I_3^-}$ is the potential energy of the redox electrolyte (- 4,80 eV) (Turhan, 2021).

Aside from $J_{sc}$, $V_{oc}$ has a considerable impact on DSSC efficacy. $V_{oc}$, known as the open circuit voltage, is defined as in Eq. (Lee et al., 2009):

$$V_{oc} = E_{LUMO} - E_{CB} \tag{9}$$

## MATERIALS and METHODS

All calculations on the dyes analyzed were performed using the Gaussian 09 software (Caricato et al., 2009) and ground state optimization of the dyes studied was obtained at the DFT/B3LYP level (A. Becke, 1993; Lee et al., 1988) and in the gas phase using the 6-311+G(d,p) (A. D. Becke, 1993) basis set. Frequency calculations were done on the examined dyes' optimized geometries at the same ground state optimization level, and it was proven that the optimized geometries were at minimal energy on the potential energy surface with no negative frequencies (Uğurlu, 2020; Ulaş, 2020). Furthermore, the absorption spectra of the dyes investigated were simulated in dichloromethane using the TD-DFT/BHandHLYP/6-311G+(d,p) level. To represent solvent effects, the polarisable continuum model of the integral equation formalism (IEF-PCM) with dichloromethane as solvent was utilized. In previous studies (Britel et al., 2023a, 2023b), the B3LYP functional with the 6-311+G(d,p) basis set and the BHandHLYP (Wazzan & Irfan, 2020) functional techniques were also shown to be appropriate for predicting absorption spectra with high accuracy when compared to experiments.

## RESULTS and DISCUSSION

### Optimised Geometry

The chemical structures of the designed dyestuffs were optimized at the DFT/6-311+G(d,p) level in the gas phase, as shown in Figure 5.

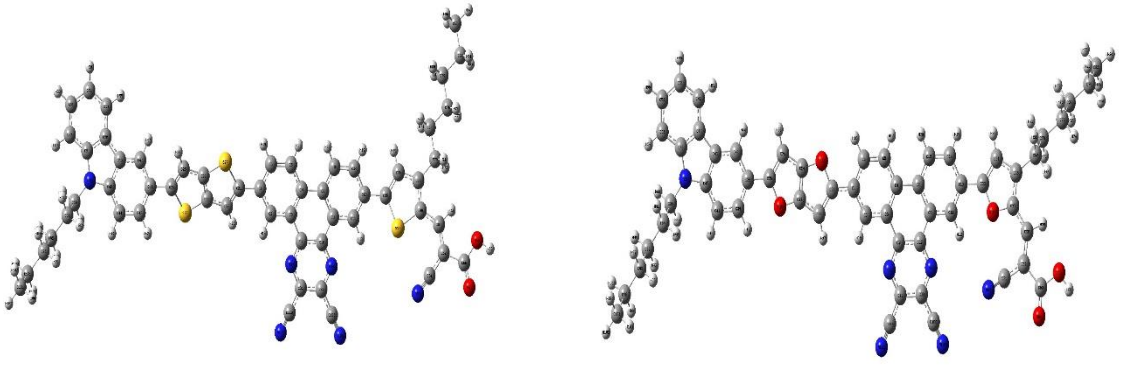

**Figure 5.** Optimised geometries of **E3** and **E4** molecules

Selected bond lengths (di) and dihedral angles (φi) are given in Table 1 and their positions in Scheme 1.

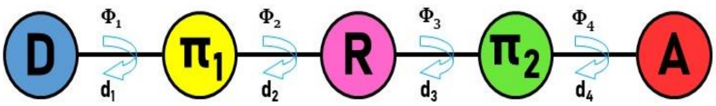

**Scheme 1.** Selected dihedral angles (**φ1**, **φ2**, **φ3**, **φ4** in °) and bond lengths (**d1**, **d2**, **d3**, **d4** in Å) of the D-π1-R-π2-A structure.

**Table 1.** Selected bond lengths (in Å) and dihedral angles (in°) of the designed structures

| | d1 (Å) | d2 (Å) | d3 (Å) | d4 (Å) | φ1 (°) | φ2(°) | φ3(°) | φ4 (°) |
|---|---|---|---|---|---|---|---|---|
| **E0** | 1.465 | ---- | ---- | 1.417 | 31.84 | ---- | ---- | -0.44 |
| | 1.465* | ---- | ---- | 1.420* | 28.21* | ---- | ---- | -0.34* |
| **E3** | 1.466 | 1.461 | 1.464 | 1.424 | -32.04 | 20.06 | -28.95 | 1.72 |
| **E4** | 1.453 | 1.446 | 1.452 | 1.414 | 0.42 | -0.02 | 10.50 | 2.99 |

*(Britel et al., 2023b)

In Table 1, bond lengths in all three structures range from 1.417 to 1.466 Å, allowing charge transfer from the carbazole donor to the cyanoacrylic acid acceptor. It shows that bond lengths decrease as one approaches from donor to acceptor and has a better conjugation effect between π2-bridge and cyanoacrylic acid. As a consequence, the excited-state electrons of all proposed structures may be efficiently injected into the $TiO_2$ conduction band. The geometry of DSSCs plays a very important role in performance. This is because the effectiveness of intramolecular charge transfer (ICT) in DSSCs is proportional to the dihedral angles between each group in the molecule. As a result, the molecule with a small dihedral angle will have greater conjugation, facilitating the ICT process. It is seen from the table that the dihedral angles of the designed structures are small.

### Electronic Structures

The charge separation is known to be intimately connected to the HOMO-LUMO distribution and to impact the performance of DSSCs. Figure 6 depicts the HOMO and LUMO distributions of the proposed dyes.

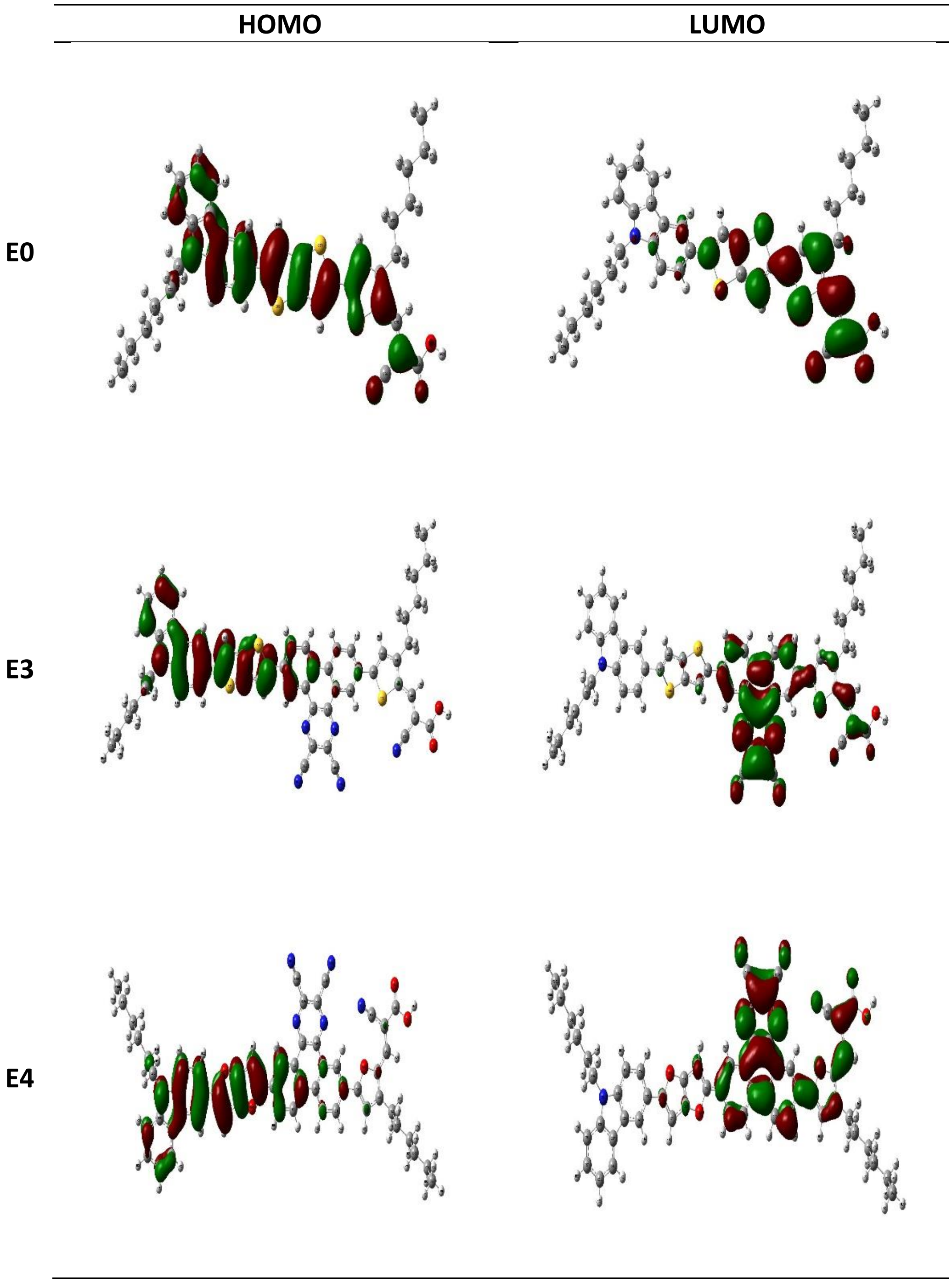

**Figure 6.** HOMO-LUMO diagrams of the optimised molecules

Looking at the HOMO diagrams, the reference structure is distributed along carbazole, thieno[3,2-b]thiophene, thiophene, and cyanoacrylic acid at **E0**. The designed **E3** and **E4** molecules were localized on carbazole and thieno[3,2-b]thiophene. In the LUMO diagrams, thieno[3,2-b]thiophene is localized along thiophene and cyanoacrylic acid for **E0**, while it is distributed in the 2,3-dicyanopyrazinophenanthrene segment in **E3** and **E4**. This indicates that load separation is achieved at **E3** and **E4**. Achieving load separation improves the ICT. This result is positive for the performance of the solar cell.

HOMO, LUMO, and the band gap are indispensable means to inject the electrons of the dyes into the conduction band of the semiconductor. Therefore, the HOMO, LUMO, and band gap energies of the optimised molecules are given in Table 2.

**Table 2.** HOMO, LUMO, and band gap energy values of the studied structures

| | $E_{homo}$ (eV) | $E_{lumo}$ (eV) | $E_{gap}$ (eV) |
|---|---|---|---|
| **E0** | -5.4707 | -2,9838 | 2,4869 |
| **E3** | -5,5257 | -3,3479 | 2,1778 |
| **E4** | -5,2729 | -3,1683 | 2,1046 |
| **$TiO_2$** | *** | -4,00 | *** |
| **$I^- /I_3^-$** | -4,80 | *** | *** |

As seen in Table 2, All structures have greater LUMO energy levels than the $TiO_2$ conduction band, but lower HOMO energy levels than the redox pair ($I^-/I_3^-$); this indicates that the injection of electrons into the $TiO_2$ conduction band and the regeneration of the dyestuff can be successfully realized (Britel et al., 2023b; Raftani et al., 2023). This result means that the HOMO and LUMO energy values do not fulfill the requirements of DSSC functionality.

The energy gap of the dye employed as a colorant in DSSCs determines its sensitivity. By boosting the molecular internal transition process, the dye with a narrow energy gap changes the absorption spectra to red and infrared and boosts the PCE of DSSC devices. These dyes have poor $E_{gap}$ values. This is most likely due to π-conjugated donor units. and π-bridge units, leading to increased charge transfer between the donor group and the acceptor group. For a molecule to be a semiconductor, its band gap must be between 0.5 eV and 4.0 eV (Atkins, 2010). The dye with the lowest band gap is **E4** (2.1046 eV). Having lower energy gaps compared to **E0** is expected to potentially lead to an absorption spectrum in the visible region. This would be beneficial to improve the $J_{sc}$ and PCE of solar cells, especially for dyes with low energy gaps.

### Nonlinear Optical Properties (NLO)

The investigation of NLO (Ugurlu & Beytur, 2020; Ulaş, 2021) characteristics is acknowledged as a useful tool for studying photovoltaic performance. Patil et al. (Patil et al., 2018) discovered that the dye had greater NLO characteristics, overall high ICT process efficiency, and improved photocurrent responsiveness, making it suitable for application as a sensitizer in high-performance photovoltaics to look at the link between structural property and NLO properties. NLO properties such as isotropic polarisability ($\alpha$) and hyperpolarisability ($\beta_{tot}$) of the studied dyes were calculated at the DFT/B3LYP/6-311+G(d,p) level and given in Table 3.

The expression for polarisability ($\alpha$) is as in Equation 10 (Zhang et al., 2010):

$$\alpha = \frac{1}{3}\left(\alpha_{xx} + \alpha_{yy} + \alpha_{zz}\right) \tag{10}$$

The tensor components of polarisability are represented by $\alpha_{xx}$, $\alpha_{yy}$, and $\alpha_{zz}$.

Third derivative of energy, (Muthu & Maheswari, 2012) It gives the total first hyperpolarisability ($\beta_{tot}$) tensor, which can be calculated using Equation 11:

$$\beta_{tot} = \sqrt{(\beta_{xxx} + \beta_{xyy} + \beta_{xzz})^2 + (\beta_{yyy} + \beta_{xxy} + \beta_{yzz})^2 + (\beta_{zzz} + \beta_{xxz} + \beta_{yyz})^2} \tag{11}$$

where $\beta_{ijk}$ ($i, j, k = x, y, z$) gives the tensor components of the hyperpolarisability.

**Table 3.** Isotropic polarisability ($\alpha$) and hyperpolarisability ($\beta_{tot}$) of the structures

| | **$\alpha$ (x$10^{-24}$ esu)** | **$\beta_{tot}$ (x$10^{-30}$ esu)** |
|---|---|---|
| **E0** | 733.62 | 56.90 |
| **E3** | 1070.58 | 101.40 |
| **E4** | 1063.88 | 141.35 |

The developed dyes have stronger isotropic polarization and hyperpolarization than the reference dye **E0**, as demonstrated in Table 3. The isotropic polarization indicates that the designed dyes may have better ICT performance than the reference dye, while the higher values of hyperpolarization suggest that they exhibit a better photocurrent response than **E0**. Based on the NLO values, it is possible to deduce that the developed dyes outperform the reference dye **E0** in photovoltaic cells.

### Electronic Absorption Spectra

The TD-BHandHLYP/6-311+G(d,p) level was used to compute the absorption characteristics in this work in order to examine the effect of adding different auxiliary groups (R) and modifying the -bridge on the optical properties of the dyes tested for DSSC. Table 4 shows the maximum absorption wavelengths ($\lambda_{max}$), oscillator powers (f), vertical excitation energies ($E_{ex}$), and transition characteristics of the dyes investigated in dichloromethane solvent.

**Table 4.** Maximum absorption wavelength ($\lambda_{max}$), vertical excitation energies ($E_{ex}$), and oscillator power (ƒ) for the investigated dyes

| | | **$\lambda_{max}$ (nm)** | **$E_{ex}$ (eV)** | **ƒ** | **Geçiş** |
|---|---|---|---|---|---|
| **E0** | **EST¹** | 486.78 | 2.547 | 1.7090 | HOMO $\longrightarrow$ LUMO (0.65) |
| | **EST²** | 338.70 | 3.661 | 0.1339 | HOMO-1 $\longrightarrow$ LUMO+1 (0.48) |
| **E3** | **EST¹** | 438.10 | 2.830 | 1.4784 | HOMO $\longrightarrow$ LUMO (0.55) |
| | **EST²** | 398.25 | 3.113 | 0.9127 | HOMO $\longrightarrow$ LUMO+1 (0.46) |
| **E4** | **EST¹** | 477.52 | 2.596 | 1.3454 | HOMO $\longrightarrow$ LUMO (0.62) |
| | **EST²** | 423.09 | 2.931 | 1.1266 | HOMO $\longrightarrow$ LUMO+1 (0.43) |

The calculated maximum absorption wavelength ($\lambda_{max}$) for **E0** is 486.78 nm, which corresponds to the measured measurement of 502 nm (Ho et al., 2021). Two transitions are important in absorption spectra: the π-π* transition and the ICT phenomenon due to charge transfer (Xu et al., 2019). The absorption bands resulting from S1 are the ICT between the electron donor and the acceptor.

As can be seen from the results, the addition of the auxiliary ligand between the π1 and π2 bridges and the change of the bridge caused a blue shift in the maximum wavelength, but the $\lambda_{max}$ values of all dyes give strong absorption bands in the visible region. This can be attributed to intramolecular charge transfer (ICT) between the donor and acceptor units. This property is useful to increase the efficiency of solar cells in converting light into electricity. The parameter known as oscillator strength (ƒ) represents the probability of absorption of electromagnetic radiation during energy level transitions of atoms or molecules. The oscillator strengths of the analyzed dyes were recorded as 1.7097, 1.4784, and 1.3454, respectively.

### Photovoltaic Properties

According to Equation (1), $J_{sc}$ and $V_{oc}$ values should be increased in order to increase PCE efficiency. $J_{sc}$, on the other hand, is highly reliant on key factors such as electron injection driving force ($\Delta G_{inj}$), light harvesting efficiency (LHE), regeneration driving force ($\Delta G_{reg}$), and total reorganization energy ($\lambda_{tot}$). As a result, a greater $J_{sc}$ guarantee can be obtained.

With the calculated $\Delta G_{inj}$, LHE, $V_{oc}$, $\Delta G_{reg}$, and $\lambda_{tot}$ values summarized in Table 5, higher-performance dyes are obtained with larger $\Delta G_{inj}$ and LHE and smaller $\Delta G_{reg}$ and $\lambda_{tot}$ values.

**Table 5.** Calculated photovoltaic parameter values

| | LHE | $V_{oc}$ (eV) | $\Delta G_{inj}$ (eV) | $\Delta G_{reg}$ (eV) | $\lambda_e$ (eV) | $\lambda_h$ (eV) | $\lambda_{tot}$ (eV) |
|---|---|---|---|---|---|---|---|
| **E0** | 0.98 | 1.0162 | -1.08 | 0.67 | 0.24 | 0.25 | 0.49 |
| **E3** | 0.97 | 0.6521 | -1.30 | 0.73 | 0.21 | 0.29 | 0.50 |
| **E4** | 0.96 | 0.8317 | -1.32 | 0.47 | 0.21 | 0.22 | 0.43 |

It depends on the LHE, which is an important parameter for evaluating the performance of organic dyestuffs. Since all LHE values of the four dyestuffs are between 0.96 and 0.98, these dyestuffs have approximately the same photoprotection.

In addition to the $J_{sc}$, open circuit voltage ($V_{oc}$) has a considerable impact on DSSC efficiency. $V_{oc}$ should be high for improved DSSC performance. The calculated $V_{oc}$ values according to Equation 9 are listed in Table 5. As can be seen from the table, the designed dyes have a lower but close $V_{oc}$ value than the reference dye, implying that they can have an almost close PCE.

A weakly negative $\Delta G_{inj}$ value and a small $\Delta G_{reg}$ value are required in acceptable sensitizers. Furthermore, a lower $\Delta G_{reg}$ is adequate to prevent recombination and reduce dyestuff degradation (Pounraj et al., 2018). From Table 5, it can be seen that the $\Delta G_{inj}$ values of all the investigated dyestuffs are negative, which can be explained by the fact that the excited state occupies the upper conduction band of $TiO_2$. This reveals that the process of injecting electrons from the dyestuff into $TiO_2$ is spontaneous. It is observed that **E0** has a larger $\Delta G_{inj}$ value (maximum value: -1.08 eV), while the values of **E3** and **E4** are small (minimum values: -1.30 eV and -1.32 eV, respectively). In this study, it shows that all designed dyestuffs, E3 and E4, have a larger electron injection driving force than **E0**. This will probably result in a high $J_{sc}$ relative to **E0**. The regeneration energy ($\Delta G_{reg}$) for any dye, on the other hand, is positive, suggesting that the sensitiser's ground state is below the electrolyte redox couple and so electron recombination is inhibited (Abdullah et al., 2013; Zhang et al., 2013). For the designed dyes, the $\Delta G_{reg}$ value of **E4** (0.47 eV) is smaller than the others, indicating that **E4** regenerates faster than the other dyes. This in turn provides the possibility of increasing $J_{sc}$ and, hence, PCE.

Charge transfer rates are crucial to the efficacy of DSSCs (Marcus, 2020). The charge transfer rate (KET) may be calculated using Marcus theory using the following equation (Chaitanya et al., 2014):

$$K_{ET} = \frac{1}{\sqrt{\lambda_{tot}}} \sqrt{\frac{\pi}{\hbar k_B\, T}}\, |V^2|\, exp\left\{-\frac{\lambda_{tot}}{4k_B T}\right\} \tag{12}$$

Here, an equation is mentioned where the charge transfer coupling is represented by V, T the absolute temperature, $\lambda_{tot}$ the rearrangement energy, and $k_B$ the Boltzmann constant. Equation 12 states that all parameters except $\lambda_{tot}$ are considered constant on the right-hand side. The $K_{ET}$ depends only on $\lambda_{\text{tot}}$, which is the sum of the reorganization energies of the vacuum ($\lambda_h$) and the electron ($\lambda_e$). The values of $\lambda_e$, $\lambda_h$, and $\lambda_{tot}$ are calculated by Equations (5), (6), and (7), respectively, and their values are given in Table 5.

While a small $\lambda_{tot}$ can accelerate carrier transport rates, a larger $\lambda_{tot}$ can do the opposite (Roy et al., 2018). Therefore, it is also necessary to calculate $\lambda_{\text{tot}}$ to analyze the relationship between $J_{\text{sc}}$ and electronic structure (Bourass et al., 2016). Therefore, a small $\lambda_{tot}$ can increase $J_{sc}$. According to the results listed in Table 5, it shows that the calculated $\lambda_{tot}$ of the designed dyes is between 0.43 eV and 0.50 eV and decreases as **E4 < E0 ≤ E3**. This shows that the dyestuff **E4** has the smallest $\lambda_{tot}$ energy. This demonstrates that the developed dyes have a superior charge transfer process and will thus give a better electron injection from the reference dye **E0** to the CB of $TiO_2$. Thus, it will improve the $J_{sc}$ and have a positive effect on the DSSC's performance.

According to all these results, it can be concluded that the designed **E3** and **E4** dyes are useful in improving the photovoltaic properties of **E4**. Regarding the $J_{sc}$ and $V_{oc}$ parameters, the designed **E4** dye can be considered an efficient candidate for use in a DSSC device.

### Chemical Reactivity Parameters

Chemical reactivity characteristics such as ionization potential (IP), electronic affinity (EA), chemical hardness (ɳ), electrophilicity index (ω), electron donating power (ω−), and electron accepting power (ω+), were computed for the dyes examined, and the results are reported in Table 6. The following parameters were used to derive chemical reactivity parameters (Roohi & Mohtamadifar, 2022):

$$IP = E_{+}^{+} - E_{0}^{0} \tag{13}$$

$$EA = E_{0}^{0} - E_{-}^{-} \tag{14}$$

$$\eta = (IP - EA)/2 \tag{15}$$

$$\omega^{+} = \frac{(IP+3EA)^2}{16(IP-EA)} \tag{16}$$

$$\omega^- = \frac{(3IP+EA)^2}{16(IP-EA)} \tag{17}$$

$$\omega = \frac{(IP+EA)^2}{4(IP-EA)} \tag{18}$$

**Table 6.** Chemical reactivity parameters of the investigated dyestuffs

| | IP | EA | η | ω⁻ | ω⁺ | ω |
|---|---|---|---|---|---|---|
| **E0** | 6,57 | 2,96 | 1,81 | 8,89 | 4,12 | 6,28 |
| **E3** | 5,76 | 2,62 | 1,57 | 7,88 | 3,69 | 5,59 |
| **E4** | 6,06 | 3,01 | 1,52 | 9,21 | 4,68 | 6,76 |

IP and EA can be defined as the energy barriers for vacancy and electron injections (Li et al., 2020a). To facilitate vacancy and electron injection, the dye should exhibit a smaller IP and a larger EA (He et al., 2017; Lu et al., 2018). From Table 6, it can be seen that the designed dyes show a lower IP compared to the **E0** reference dye. However, only **E4** has larger EA values compared to **E0**, which results in easier injection of vacancies and electrons into these designed dyes compared to **E0**.

A molecule's chemical stiffness is assessed by its resistance to transmitting charge to its surroundings. The η value of a dye is a measure of its capacity to transmit electrons or holes; smaller values indicate better ability. As demonstrated in Table 6, the proposed dyes have improved charge transfer capabilities due to lower η values of **E4** when compared to the reference dye **E0**.

The electrophilicity index ($\omega$) is a measure of molecular structure stabilization energies; the higher the $\omega^+$ value, the greater the electron acceptance; hence, larger $\omega$ and $\omega^+$ values are preferred. The results obtained in Table 6 reveal that **E4** of the designed dyes has the highest electron acceptance and stabilization energy among the E0 reference dyes. In addition, the calculated $\omega^-$ values show the same trend as $\omega^+$, and it is concluded that the designed **E4** dye exhibits better electron-donating ability than the reference dye.

According to the above discussion, among the designed dyes, **E4** has the best charge transferability, highest stabilisation energy, and best electron donating and electron accepting ability. As a result, it has a higher power conversion energy (PCE) and a higher short-circuit current than the reference dye **E0**.

## Competing interest statement

The authors declare no conflic to finterest.

## Additional information

No additional information is available for this paper.

## REFERENCES

Abdullah, M. I., Janjua, M. R. S. A., Mahmood, A., Ali, S., & Ali, M. (2013). Quantum chemical designing of efficient sensitizers for dye sensitized solar cells. *Bulletin of the Korean Chemical Society*, *34*(7), 2093-2098.

Atkins, P. (2010). *Shriver and Atkins' inorganic chemistry*. Oxford University Press, USA.

Becke, A. (1993). Density-Functional Thermochemistry. III. The Role of Exact Exchange. J. Chem. Phys., 98: 5648-5652. In.

Becke, A. D. (1993). A new mixing of Hartree–Fock and local density-functional theories. *The Journal of chemical physics*, *98*(2), 1372-1377.

Bomben, P. G., Robson, K. C., Koivisto, B. D., & Berlinguette, C. P. (2012). Cyclometalated ruthenium chromophores for the dye-sensitized solar cell. *Coordination Chemistry Reviews*, *256*(15-16), 1438-1450.

Bourass, M., Benjelloun, A. T., Benzakour, M., Mcharfi, M., Hamidi, M., Bouzzine, S., Serein-Spirau, F., Jarrosson, T., Lère-Porte, J., & Sotiropoulos, J.-M. (2016). The computational study of the electronic and optoelectronics properties of new materials based on thienopyrazine for application in dye solar cells. *Journal of Materials and Environmental Science*, *7*(3), 700-712.

Britel, O., Fitri, A., Benjelloun, A. T., Benzakour, M., & Mcharfi, M. (2023a). Carbazole based D-πi-π-A dyes for DSSC applications: DFT/TDDFT study of the influence of πi-spacers on the photovoltaic performance. *Chemical Physics*, *565*, 111738.

Britel, O., Fitri, A., Benjelloun, A. T., Benzakour, M., & Mcharfi, M. (2023b). New carbazole-based dyes for efficient dye-sensitized solar cells: a DFT insight. *Structural Chemistry*, 1-16.

Caricato, M., Frisch, M. J., Hiscocks, J., & Frisch, M. J. (2009). *Gaussian 09: IOps Reference*. Gaussian Wallingford, CT, USA.

Chaitanya, K., Ju, X.-H., & Heron, B. M. (2014). Theoretical study on the light harvesting efficiency of zinc porphyrin sensitizers for DSSCs. *RSC advances*, *4*(51), 26621-26634.

Dutta, R., Ahmed, S., & Kalita, D. J. (2020). Theoretical design of new triphenylamine based dyes for the fabrication of DSSCs: A DFT/TD-DFT study. *Materials Today Communications*, *22*, 100731.

Fitri, A., Benjelloun, A. T., Benzakour, M., Mcharfi, M., Hamidi, M., & Bouachrine, M. (2014a). Theoretical design of thiazolothiazole-based organic dyes with different electron donors for dye-sensitized solar cells. *Spectrochimica Acta Part A: Molecular and Biomolecular Spectroscopy*, *132*, 232-238.

Fitri, A., Benjelloun, A. T., Benzakour, M., Mcharfi, M., Hamidi, M., & Bouachrine, M. (2014b). Theoretical investigation of new thiazolothiazole-based D-π-A organic dyes for efficient dye-sensitized solar cell. *Spectrochimica Acta Part A: Molecular and Biomolecular Spectroscopy*, *124*, 646-654.

Grätzel, M. (2001). Photoelectrochemical cells. *nature*, *414*(6861), 338-344.

Hamann, T. W., Jensen, R. A., Martinson, A. B., Van Ryswyk, H., & Hupp, J. T. (2008). Advancing beyond current generation dye-sensitized solar cells. *Energy & Environmental Science*, *1*(1), 66-78.

He, L.-J., Wang, J., Chen, J., Jia, R., & Zhang, H.-X. (2017). The effect of relative position of the π-spacer center between donor and acceptor on the overall performance of D-π-A dye: a theoretical study with organic dye. *Electrochimica Acta*, *241*, 440-448.

Higashino, T., & Imahori, H. (2015). Porphyrins as excellent dyes for dye-sensitized solar cells: recent developments and insights. *Dalton transactions*, *44*(2), 448-463.

Ho, P.-Y., Wang, Y., Yiu, S.-C., Kwok, Y.-Y., Siu, C.-H., Ho, C.-L., Lee, L. T. L., & Chen, T. (2021). Photophysical characteristics and photosensitizing abilities of thieno [3, 2-b] thiophene-Based photosensitizers for photovoltaic and photocatalytic applications. *Journal of Photochemistry and Photobiology A: Chemistry*, *406*, 112979.

Huang, R.-Y., Tsai, W.-H., Wen, J.-J., Chang, Y. J., & Chow, T. J. (2020). Spiro [fluorene-9, 9′-phenanthren]-10′-one as auxiliary acceptor of DA-π-A dyes for dye-sensitized solar cells under one sun and indoor light. *Journal of Power Sources*, *458*, 228063.

Ibrahim, M. M., El-Shafai, N. M., El-Mehasseb, I. M., Abdou, S. N., & El-Sheshtawy, H. S. (2021). Tuning optical properties of triphenylamine-pyrrole by alkyl-substituted thiobarbituric acid for dye-sensitized solar cell. *International Journal of Energy Research*, *45*(10), 14804-14812.

Kumar, A., Richhariya, G., & Sharma, A. (2015). Solar photovoltaic technology and its sustainability. *Energy sustainability through green energy*, 3-25.

Lee, C., Yang, W., & Parr, R. G. (1988). Development of the Colle-Salvetti correlation-energy formula into a functional of the electron density. *Physical review B*, *37*(2), 785.

Lee, W., Roh, S.-J., Hyung, K.-H., Park, J., Lee, S.-H., & Han, S.-H. (2009). Photoelectrochemically polymerized polythiophene layers on ruthenium photosensitizers in dye-sensitized solar cells and their beneficial effects. *Solar Energy*, *83*(5), 690-695.

Li, Y., Li, X., & Xu, Y. (2020a). A rational design of excellent light-absorbing dyes with different N-substituents at the phenothiazine for high efficiency solar cells. *Spectrochimica Acta Part A: Molecular and Biomolecular Spectroscopy*, *234*, 118241.

Li, Y., Li, X., & Xu, Y. (2020b). Theoretical screening of high-efficiency sensitizers with D-π-A framework for DSSCs by altering promising donor group. *Solar Energy*, *196*, 146-156.

Li, Y., Liu, J., Liu, D., Li, X., & Xu, Y. (2019). DA-π-A based organic dyes for efficient DSSCs: A theoretical study on the role of π-spacer. *Computational Materials Science*, *161*, 163-176.

Liang, M., & Chen, J. (2013). Arylamine organic dyes for dye-sensitized solar cells. *Chemical Society Reviews*, *42*(8), 3453-3488.

Lu, T.-F., Li, W., Chen, J., Tang, J., Bai, F.-Q., & Zhang, H.-X. (2018). Promising pyridinium ylide based anchors towards high-efficiency dyes for dye-sensitized solar cells applications: Insights from theoretical investigations. *Electrochimica Acta*, *283*, 1798-1805.

Mandal, S., Kandregula, G. R., & Ramanujam, K. (2020). Replacing aromatic π-system with cycloalkyl in triphenylamine dyes to impact intramolecular charge transfer in dyes pertaining to dye-sensitized solar cells application. *Journal of Photochemistry and Photobiology A: Chemistry*, *403*, 112862.

Marcus, R. A. (2020). Electron transfer reactions in chemistry. Theory and experiment. In *Protein electron transfer* (pp. 249-272). Garland Science.

Marlina, L. A., Haryadi, W., Daengngern, R., & Pranowo, H. D. (2022). Molecular design of benzo [c][1, 2, 5] thiadiazole or thieno [3, 4-d] pyridazine-based auxiliary acceptors through different anchoring groups in D-π-AA framework: A DFT/TD-DFT study. *Journal of Molecular Graphics and Modelling*, *113*, 108148.

Mathew, S., Yella, A., Gao, P., Humphry-Baker, R., Curchod, B. F., Ashari-Astani, N., Tavernelli, I., Rothlisberger, U., Nazeeruddin, M. K., & Grätzel, M. (2014). Dye-sensitized solar cells with 13% efficiency achieved through the molecular engineering of porphyrin sensitizers. *Nature chemistry*, *6*(3), 242-247.

Mersal, G. A., Toghan, A., Yahia, I. S., & El-Sheshtawy, H. S. (2021). Pyrrole/thiophene π-bridged two triphenylamine electron donor and substituted thiobarbituric electron acceptor for D-π-A-D-featured DSSC applications. *Journal of the Chinese Chemical Society*, *68*(10), 1842-1851.

Muthu, S., & Maheswari, J. U. (2012). Quantum mechanical study and spectroscopic (FT-IR, FT-Raman, 13C, 1H, UV) study, first order hyperpolarizability, NBO analysis, HOMO and LUMO analysis of 4-[(4-aminobenzene) sulfonyl] aniline by ab initio HF and density functional method. *Spectrochimica Acta Part A: Molecular and Biomolecular Spectroscopy*, *92*, 154-163.

Noh, H. J., Ji, J.-M., Hwang, S. P., Kim, C. H., & Kim, H. K. (2021). D-π-A-structured organic sensitizers with π-extended auxiliary acceptor units for high-performance dye-sensitized solar cells. *Dyes and Pigments*, *195*, 109681.

O'regan, B., & Grätzel, M. (1991). A low-cost, high-efficiency solar cell based on dye-sensitized colloidal TiO2 films. *nature*, *353*(6346), 737-740.

Patil, D. S., Avhad, K. C., & Sekar, N. (2018). Linear correlation between DSSC efficiency, intramolecular charge transfer characteristics, and NLO properties–DFT approach. *Computational and Theoretical Chemistry*, *1138*, 75-83.

Pounraj, P., Mohankumar, V., Pandian, M. S., & Ramasamy, P. (2018). Donor functionalized quinoline based organic sensitizers for dye sensitized solar cell (DSSC) applications: DFT and TD-DFT investigations. *Journal of Molecular Modeling*, *24*, 1-23.

Raftani, M., Abram, T., Azaid, A., Kacimi, R., Bennani, M., & Bouachrine, M. (2023). New organic dyes with low bandgap based on heterocyclic compounds for dye-sensitized solar cells applications. *Biointerface Research in Applied Chemistry*, *13*.

Roohi, H., & Mohtamadifar, N. (2022). The role of the donor group and electron-accepting substitutions inserted in π-linkers in tuning the optoelectronic properties of D–π–A dye-sensitized solar cells: a DFT/TDDFT study. *RSC advances*, *12*(18), 11557-11573.

Roy, J. K., Kar, S., & Leszczynski, J. (2018). Insight into the optoelectronic properties of designed solar cells efficient tetrahydroquinoline dye-sensitizers on TiO2 (101) surface: first principles approach. *Scientific Reports*, *8*(1), 10997.

Saad Ebied, M., Dongol, M., Ibrahim, M., Nassary, M., Elnobi, S., & Abuelwafa, A. A. (2022). Effect of carboxylic acid and cyanoacrylic acid as anchoring groups on Coumarin 6 dye for dye-sensitized solar cells: DFT and TD-DFT study. *Structural Chemistry*, *33*(6), 1921-1933.

Singh, M., & Kanaparthi, R. K. (2022). Theoretical exploration of 1, 3-Indanedione as electron acceptor-cum-anchoring group for designing sensitizers towards DSSC applications. *Solar Energy*, *237*, 456-469.

Tan, L.-L., Huang, J.-F., Shen, Y., Xiao, L.-M., Liu, J.-M., Kuang, D.-B., & Su, C.-Y. (2014). Highly efficient and stable organic sensitizers with duplex starburst triphenylamine and carbazole donors for liquid and quasi-solid-state dye-sensitized solar cells. *Journal of Materials Chemistry A*, *2*(24), 8988-8994.

Tripathi, A., Kumar, V., & Chetti, P. (2022). Impact of internal (donor/acceptor) moieties and π-spacer in triphenylamine-based dyes for DSSCs. *Journal of Photochemistry and Photobiology A: Chemistry*, *426*, 113738.

Turhan, Z. Ş. (2021). Fenazin Tabanlı Bileşiklerin OLED ve TADF Özelliklerinin İncelenmesi. *Journal of the Institute of Science and Technology*, *11*(4), 2926-2936.

Ugurlu, G., & Beytur, M. (2020). Theoretical studies on the structural, vibrational, conformational analysis and nonlinear optic property of 4-(methoxycarbonyl)-phenylboronic acid. *Indian Journal Of Chemistry Section A-Inorganic Bio-Inorganic Physical Theoretical & Analytical Chemistry*, *59*(10), 1504-1512.

Uğurlu, G. (2020). Ortorombik metaborik asit molekülünün moleküler yapısı ve elektronik özellikleri üzerindeki konformasyonel etkinin teorik olarak incelenmesi. *Journal of Boron*, *5*(2), 91-99.

Ulaş, Y. (2020). Experimental and Theoretical Studies of 2-(naphthalen-1-yl (piperidin-1-yl) methyl) phenol Compound. *J. Chem. Soc. Pak*, *42*(6), 818-826.

Ulaş, Y. (2021). Investigation of the relationship between the substituent and nonlinear optical properties in 2-(Phenyl ((4-Vinylphenyl) Amino) Methyl) phenol derivative compounds by DFT method. *Journal of the Chemical Society of Pakistan*, *43*(3), 271-277.

Wazzan, N., & Irfan, A. (2020). Promising architectures modifying the D-π-A architecture of 2, 3-dipentyldithieno [3, 2-f: 2′, 3′-h] quinoxaline-based dye as efficient sensitizers in dye-sensitized solar cells: a DFT study. *Materials Science in Semiconductor Processing*, *120*, 105260.

Xu, Z., Li, Y., Zhang, W., Yuan, S., Hao, L., Xu, T., & Lu, X. (2019). DFT/TD-DFT study of novel T shaped phenothiazine-based organic dyes for dye-sensitized solar cells applications. *Spectrochimica Acta Part A: Molecular and Biomolecular Spectroscopy*, *212*, 272-280.

Yang, Z., Liu, C., Li, K., Cole, J. M., Shao, C., & Cao, D. (2018). Rational design of dithienopicenocarbazole-based dyes and a prediction of their energy-conversion efficiency characteristics for dye-sensitized solar cells. *ACS Applied Energy Materials*, *1*(4), 1435-1444.

Zhang, C.-R., Liu, L., Zhe, J.-W., Jin, N.-Z., Ma, Y., Yuan, L.-H., Zhang, M.-L., Wu, Y.-Z., Liu, Z.-J., & Chen, H.-S. (2013). The role of the conjugate bridge in electronic structures and related properties of tetrahydroquinoline for dye sensitized solar cells. *International journal of molecular sciences*, *14*(3), 5461-5481.

Zhang, R., Du, B., Sun, G., & Sun, Y. (2010). Experimental and theoretical studies on o-, m-and p-chlorobenzylideneaminoantipyrines. *Spectrochimica Acta Part A: Molecular and Biomolecular Spectroscopy*, *75*(3), 1115-1124.

Zhang, Z., Hu, W., He, R., Shen, W., & Li, M. (2017). The influence of inserted thiophene into the (π-A'-π)-bridge on photovoltaic performances of dye-sensitized solar cells. *Materials Chemistry and Physics*, *191*, 121-128.